Chinese Journal of Natural Medicines

Chiral resolution of furofuran lignans and their derivatives from the stems of *Dendrobium* 'Sonia'

Kaimei QIU, Hao QIU, Yanqiao XIE, Siyu ZHANG, Qian ZHANG, Zhengtao WANG, Zhuzhen HAN, Li YANG

Citation: Kaimei QIU, Hao QIU, Yanqiao XIE, Siyu ZHANG, Qian ZHANG, Zhengtao WANG, Zhuzhen HAN, Li YANG, Chiral resolution of furofuran lignans and their derivatives from the stems of *Dendrobium* 'Sonia', Chinese Journal of Natural Medicines, 2024, 22(10), 937−944. doi: 10.1016/S1875−5364(24)60725−9.

View online: https://doi.org/10.1016/S1875−5364(24)60725−9

Available online at www.sciencedirect.com
ScienceDirect
Chinese Journal of Natural Medicines 2024, **22**(10): 937-944
doi: 10.1016/S1875-5364(24)60725-9
Chinese Journal of Natural Medicines

•Original article•

Chiral resolution of furofuran lignans and their derivatives from the stems of *Dendrobium* 'Sonia'

QIU Kaimei, QIU Hao, XIE Yanqiao, ZHANG Siyu, ZHANG Qian, WANG Zhengtao, HAN Zhuzhen*, YANG Li*

The MOE Key Laboratory of Standardization of Chinese Medicines, The SATCM Key Laboratory of New Resources and Quality Evaluation of Chinese Medicines, The Shanghai Key Laboratory for Compound Chinese Medicines, Institute of Chinese Materia Medica, Shanghai University of Traditional Chinese Medicine, Shanghai 201203, China

Available online 20 Oct., 2024

[ABSTRACT] Five new furofuran lignans and their derivatives, (−)-glaberide I 4-*O*-*β*-D-glucopyranoside (**1a**), (+)-glaberide I 4-*O*-*β*-D-glucopyranoside (**1b**), (+)-glaberide I 7'-ethoxy-4-*O*-*β*-D-glucopyranoside (**2a**), (−)-glaberide I 7'-ethoxy-4-*O*-*β*-D-glucopyranoside (**2b**), and (−)-isoeucommin A (**3b**), along with fifteen known analogs were isolated from the stems of *Dendrobium* 'Sonia'. These compounds were classified into ten pairs of enantiomers or diastereoisomers *via* chiral resolution, and their structures were determined based on extensive spectroscopic data. Their absolute configurations were determined by hydrolysis, comparison of experimental and calculated electronic circular dichroism (ECD) data, and single-crystal X-ray diffraction analysis. The isolates were evaluated for their ability to inhibit nitric oxide (NO) production in RAW264.7 cells. Among them, syringaresinol (**5**) exhibited prominent inhibition activity, with an IC_{50} value of 28.4 ± 3.0 μmol·L^{-1}, and there was a slight difference between **5a**, **5b** and the racemic mixture **5**.

[KEY WORDS] Furofuran lignans; Chiral resolution; Enantiomers; Diastereoisomers; *Dendrobium* 'Sonia'; Anti-inflammatory
[CLC Number] R284.1 **[Document code]** A **[Article ID]** 2095-6975(2024)10-0937-08

Introduction

Dendrobium (Orchidaceae), known as 'Shihu', has a long history of use in traditional Chinese medicine for its stomachic benefits, promotion of body fluid production, and heat-clearing properties. In recent decades, the medicinal chemistry of *Dendrobium* spp. has become a hot-spot research area. Numerous studies have shown that *Dendrobium* plants are rich in a variety of natural products, including bibenzyls [1, 2], phenanthrenes [3], lignans [4, 5], sesquiterpenes [6], alkaloids [7], polysaccharides [8], and flavonoids [9, 10].

Dendrobium 'Sonia', an artificially cultivated hybrid from the Orchidaceae family [11], is used in China similarly to traditional 'Shihu'. However, most research on *Dendrobium* 'Sonia' has focused on tissue culture, with limited exploration of its phytochemical components. Our team has led pioneering studies on the phytochemistry of this hybrid. In the initial phase, we focused on stilbenes and reported two novel phenylpropanoid derivatives [12] and two new stilbenoid diglycosides [13]. A comprehensive literature review revealed that *Dendrobium* spp. is particularly rich in lignans, which often exist as chiral isomers and exhibit various biological effects, such as anti-oxidant [14], anti-inflammatory [15] and anti-bacterial [16] activities.

Our research identified the presence of racemates through the cleavage phenomenon observed in ^{13}C NMR spectra. Subsequent experiments facilitated the chiral resolution and absolute configuration determination of ten pairs of furofuran lignans and their derivatives (**1**−**10**, Fig. 1), yielding five new stereoisomeric compounds (**1a**, **1b**, **2a**, **2b**, and **3b**). The furofuran lignan or norlignan nucleus can be classified into four groups, each existing as enantiomeric isomers, with their derivatives being diastereoisomers due to opposite configurations at the chiral centers in the aglycone fragments. Our findings demonstrated that compounds with absolute configurations of 7*R*, 8*S*, 8'*S* exhibited negative peaks in circular dichroism (CD) curves in the range of 200–250 nm and had negative optical rotation values. In contrast, compounds with configurations of 7*S*, 8*R*, 8'*R* displayed opposite CD results. Furthermore, the compounds were evaluated for their inhibition against nitric oxide (NO) production. Among them,

[Received on] 07-Nov.-2023
[Research funding] This work was financially supported by the Program of Shanghai Municipal Commission of Health and Family Planning [No. ZY (2021-2023)-0215].
[*Corresponding author] E-mails: hltang@126.com (HAN Zhuzhen); yl7@shutcm.edu.cn (YANG Li)
These authors have no conflict of interest to declare.

syringaresinol (**5**) showed significant anti-inflammatory activity with an IC_{50} value of 28.4 ± 3.0 μmol·L^{-1}. Specifically, the levorotatory enantiomer **5a** (IC_{50} 26.9 ± 3.5 μmol·L^{-1}) was slightly more active than the racemic mixture, while the dextrorotatory enantiomer **5b** (IC_{50} 35.5 ± 1.1 μmol·L^{-1}) was slightly less active. These minor differences in anti-inflammatory activity among the enantiomers may serve as a basis for clinical application

Results and Discussion

Structural analysis

Compound **1** was obtained as a white solid. The HR-ESI-MS showed an $[M - H]^-$ peak at *m/z* 441.1401 (Calcd. for *m/z* 441.1402), establishing the molecular formula as $C_{20}H_{26}O_{11}$, supported by ^{13}C NMR data. The ^1H NMR spectrum (Table 1) indicated aromatic proton signals characteristic of a 1,3,4,5-tetrasubstituted benzene ring [δ_H 6.79 (2H, s, H-2/6)], two methoxyl groups attached to the benzene ring [δ_H 3.86 (6H, s, 3/5-OCH_3)], and a *β*-glucose terminal hydrogen proton signal [δ_H 5.02 (1H, m, H-1")]. The ^{13}C NMR and DEPT spectra identified carbon signals, including one ester carbonyl signal at δ_C 182.0 (C-7'), aromatic carbon signals at δ_C 152.6 (C-3/5), 136.5 (C-4), 133.2 (C-1), and 103.9 (C-2/6), hexose signals at δ_C 102.9 (C-1"), 73.6 (C-2"), 75.6 (C-3"), 69.2 (C-4"), 76.3 (C-5"), and 60.4 (C-6"), two methoxyl signals at δ_C 56.2 (3/5-OCH_3), two oxymethylene signals at δ_C 71.6 (C-9') and 69.7 (C-9), and three methylene signals at δ_C 85.9 (C-7), 47.5 (C-8), and 46.4 (C-8'). The key HMBCs of H-7/C-1 and C-8 indicated linkage between C-1 and C-7, while the HMBCs of H-8'/C-7' verified the carbonyl at C-7'. The above NMR data indicated that **1** was a norlignan glucoside. Moreover, the hexose moiety was confirmed as D-glucose *via* GC-MS analysis after acid hydrolysis and derivatization. Comprehensive interpretation of 2D NMR spectra established the gross structure of **1** as glaberide I 4-*O*-*β*-D-glucopyranoside [17]. The NOESY correlations of H-8/H-8' indicated that H-8 and H-8' were on the same face, while the correlations of H-2/H-8 indicated that H-7 was on the opposite face, determining the relative configuration of compound **1**. However, the detailed observation of its ^{13}C NMR spectrum revealed twin peaks for most carbon signals, suggesting that **1** exists as a pair of isomers. After separated by chiral-phase HPLC, **1a** and **1b** were successfully isolated, with their spin values at $[\alpha]_D^{20}$−59.2 (*c* 0.1, MeOH) and $[\alpha]_D^{20}$+49.5 (*c* 0.1, MeOH), respectively. Hydrolysis followed by EtOAc extraction of **1a** indicated that the retention time of its aglycone part matched that of (−)-dendrolactone (**4a**) under the same HPLC conditions using a chiral column (Fig. 2). In addition, the experimental CD curves of **1a** and **1b** were closely matched those of (−)-dendrolactone (**4a**) and (+)-dendrolactone (**4b**), respectively. Furthermore, a comparison of the experimental and calculated ECD curves (Fig. 4) confirmed the absolute configuration of **1a** as (−)-glaberide I 4-*O*-*β*-D-glucopyranoside (7*R*, 8*S*, 8'*S*). Similarly, **1b** was identified as (+)-glaberide I 4-*O*-*β*-D-glucopyranoside (7*S*, 8*R*, 8'*R*) based on its complementary CD curves to those of **1a**. Therefore, the structures of **1a** and **1b** were established, as shown in Fig. 3.

Compound **2** was obtained as a white solid. Its molecular formula, $C_{22}H_{32}O_{11}$, was assigned based on the HR-ESI-MS data, which showed an $[M - H]^-$ ion at *m/z* 471.1876 (Calcd. for *m/z* 471.1871). The high abundance of its secondary mass spectral fragment at *m/z* 175.0401 implied structural similarities to known norlignan compounds, such as **1** and **4**. The ^1H NMR data of **2** closely resembled those of **1**, revealing signals for a 1,3,4,5-tetrasubstituted benzene ring, one overlapping methoxy group, and a *β*-glucose terminal hydrogen proton signal (Table 1). Additionally, a hemiketal hydrogen proton signal [δ_H 4.99 (1H, brs, H-7')] and an ethoxy group [δ_H 1.18 (3H, t, *J* = 7.07 Hz, H-10), δ_C 15.6 (C-10); δ_H 3.69 (1H, overlapped, H-11a), δ_H 3.45 (1H, overlapped, H-11b), δ_C 63.8 (C-11)] were identified, which were further confirmed by HSQC and ^1H-^1H COSY data. The ^{13}C NMR and DEPT spectra revealed twenty-two carbon signals, including three methyl, four methylene, eleven hypomethyl, and four quaternary carbon signals, consistent with a typical furofuran norligan glucoside. The HMBCs of H-1"/C-4 confirmed the glucose attachment at C-4, and the HMBCs of H-7',10/C-11 verified the presence of an ethoxy group at C-7'. This structure was consistent with literature reports of lignans containing ethoxy groups [18]. Similarly, the *β*-D-glucose moiety was confirmed through hydrolytic derivatization and GC-MS analysis. Based on these findings, the planar structure of **2** was elucidated as glaberide I 7'-ethoxy-4-*O*-*β*-D-glucopyranoside [18]. For the absolute configuration of **2**, the optical rotation value for **2b** was −51.6 (*c* 0.1, MeOH), and its CD curve was nearly identical to that of (−)-syringaresinol (**5b**). In the NOESY spectrum, the absence of correlation between H-7 and H-8' was consistent with the similar compound (−)-dendrolactone (**4a**), suggesting an absolute configuration of 7*R*, 8*S*, 8'*S*. Furthermore, the NOESY correlation of H-7/H-7' disclosed that H-7' was on the same face as H-7. DP4$^+$ calculations showed that the calculated chemical shift values closely matched the measured values when the absolute configuration of C-7' was *R*. Finally, the comparison between the calculated ECD curves and the experimental ones confirmed the absolute configuration of **2a** as (+)-glaberide I 7'-ethoxy-4-*O*-*β*-D-glucopyranoside (7*S*,8*R*, 7'*S*,8'*R*). Thus, the absolute configuration of **2b** was defined as (−)-glaberide I 7'-ethoxy-4-*O*-*β*-D-glucopyranoside (7*R*, 8*S*,7'*R*,8'*S*) due to its nearly opposite CD curves compared with **2a**. The structures of **2a** and **2b** were established, as shown in Fig. 3.

Compound **3** was isolated as a white solid. Its molecular formula was determined to be $C_{27}H_{34}O_{12}$ based on the ion at *m/z* 549.1980 $[M - H]^-$ (Calcd. for *m/z* 549.1977) in the HR-ESI-MS data and ^{13}C NMR spectra. The 1D NMR spectra of **3** were similar to those of **2**, with the addition of signals for a glucose moiety and an extra aromatic ring (Table 1). These characteristics closely matched those of the known natural compound isoeucommin A [19] (also known as medioresinol-4'-

Table 1 ^{1}H (400 MHz) and ^{13}C (100 MHz) NMR spectral data for **1ab**, **2ab**, and **3b**

No.	1ab (D_2O)		2ab (CD_3OD)		3b (CD_3OD)	
	δ_H (*J* in Hz)	δ_C	δ_H (*J* in Hz)	δ_C	δ_H (*J* in Hz)	δ_C
1		133.2		139.4		136.1
2/6	6.79 (2H, s)	103.9	6.71 (2H, s)	105	6.66 (2H, s)	104.7
3/5		152.6		154.6		149.5
4		136.5		135.8		134.8
7	4.83 (1H, ov)	85.9	4.40 (1H, ov)	88.6	4.72 (1H, d, 4.3)	87.8
8	3.37 (1H, ov)	47.5	2.84 (1H, m)	54.4	3.14 (1H, m)	55.6
9	4.63 (1H, dd, 9.9, 6.8)	69.7	3.98 (1H, dd, 9.1, 5.9)	70.2	4.27 (1H, ov)	73.0
	4.49 (1H, dd, 9.9, 1.7)		3.96 (1H, dd, 9.1, 1.2)		3.90 (1H, ov)	
7'		182.0	4.99 (1H, brs)	108.7	4.77 (1H, d, 3.9)	87.2
8'	3.71 (1H, ov)	46.4	3.03 (1H, m)	54.3	3.14 (1H, m)	55.7
9'	3.61 (1H, m)	71.6	4.35 (1H, ov)	72.6	4.27 (1H, ov)	72.9
	4.19 (1H, dd, 9.4, 3.3)		4.40 (1H, dd)		3.90 (1H, ov)	
10			1.18 (3H, t, 7.07)	15.6		
11			3.69 (1H, ov)	63.8		
			3.45 (1H, ov)			
3/5-OCH_3	3.86 (6H, s)	56.2	3.87 (6H, s)	57.2	3.85 (6H, s)	57.0
1'						131.7
2'					7.04 (1H, d, 1.8)	111.8
3'						151.2
4'						147.7
5'					7.15 (1H, d, 8.3)	118.2
6'					6.93 (1H, dd, 8.4, 1.8)	120.0
3'-OCH_3					3.87 (3H, s)	56.9
1"	5.02 (1H, m)	102.9	4.86 (1H, dd, 7.52, 1.1)	105.5	4.88 (1H, ov)	103.0
2"	3.55 (1H, ov)	73.6	4.37 (1H, ov)	75.8	3.49 (1H, ov)	75.1
3"	3.54 (1H, ov)	75.6	3.41 (1H, ov)	78.0	3.46 (1H, ov)	78.0
4"	3.48 (1H, ov)	69.2	3.41 (1H, ov)	71.5	3.39 (1H, ov)	71.5
5"	3.33 (1H, ov)	76.3	3.20 (1H, m)	78.5	3.39 (1H, ov)	78.4
6"	3.80 (1H, dd, 12.4, 2.1)	60.4	3.77 (1H, dd, 11.9, 2.4)	62.7	3.86 (1H, dd, 12.0, 2.36)	62.7
	3.71 (1H, ov)		3.68 (1H, ov)		3.68 (1H, ov)	

Note: ov is the abbreviation of overlapped.

O-*β*-D-glucopyranoside). Closer inspection of the ^{13}C NMR spectrum revealed minor separations in some carbon signals, suggesting that **3** existed as a mixture of a pair of isomers. Fortunately, utilizing a chiral CD-Ph column, **3** was successfully separated into two individual isomers, designated as **3a** and **3b**. The absolute configuration of **3a** was confirmed as (−)-isoeucommin A (7*S*,8*R*,7'*S*,8'*R*) [19] through ECD calculations. Accordingly, the absolute configuration of **3b** could be determined as well. Collectively, the structure of **3a** was established as isoeucommin A (7*S*,8*R*,7'*S*,8'*R*) and **3b** as isoeucommin A (7*R*,8*S*,7'*R*,8'*S*), as shown in Fig. 3.

Additionally, fifteen known furofuran lignans and their derivatives were isolated and identified as (−)-dendrolactone (7*R*,8*S*,8'*S*) (**4a**) [20-22], (+)-dendrolactone (7*S*,8*R*,8'*R*) (**4b**) [21]; (+)-syringaresinol (7*S*,8*R*,7'*S*,8'*R*) (**5a**), (−)-syringaresinol (7*R*,8*S*,7'*R*,8'*S*) (**5b**) [23]; (+)-medioresinol (7*S*,8*R*,7'*S*,8'*R*) (**6a**), (−)-medioresinol (7*R*,8*S*,7'*R*,8'*S*) (**6b**) [24]; (−)-syringaresinol-*O*-*β*-D-glucoside (7*R*,8*S*,7'*R*,8'*S*) (**7a**), (+)-syr-

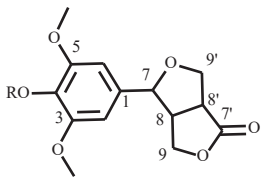

1a* (7*R*, 8*S*, 8'*S*), R = *β*-D-glu
1b* (7*S*, 8*R*, 8'*R*), R = *β*-D-glu
4a (7*R*, 8*S*, 8'*S*), R = H
4b (7*S*, 8*R*, 8'*R*), R = H

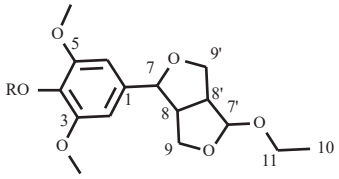

2a* (7*S*, 8*R*, 7'*S*, 8'*R*), R = *β*-D-glu
2b* (7*R*, 8*S*, 7'*R*, 8'*S*), R = *β*-D-glu

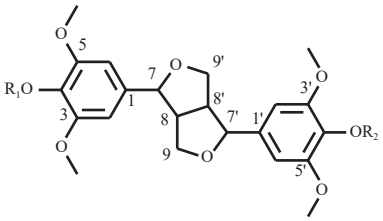

5a (7*S*, 8*R*, 7'*S*, 8'*R*), R_1 = H, R_2 = H
5b (7*R*, 8*S*, 7'*R*, 8'*S*), R_1 = H, R_2 = H
7a (7*R*, 8*S*, 7'*R*, 8'*S*), R_1 = H, R_2 = *β*-D-glu
7b (7*S*, 8*R*, 7'*S*, 8'*R*), R_1 = H, R_2 = *β*-D-glu
9a (7*S*, 8*R*, 7'*S*, 8'*R*), R_1 = *β*-D-glu, R_2 = *β*-D-glu
9b (7*R*, 8*S*, 7'*R*, 8'*S*), R_1 = *β*-D-glu, R_2 = *β*-D-glu

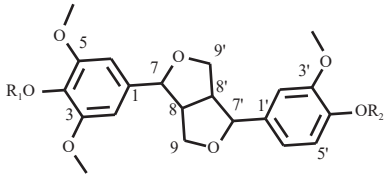

3a (7*S*, 8*R*, 7'*S*, 8'*R*), R_1 = H, R_2 = *β*-D-glu
3b* (7*R*, 8*S*, 7'*R*, 8'*S*), R_1 = H, R_2 = *β*-D-glu
6a (7*S*, 8*R*, 7'*S*, 8'*R*), R_1 = H, R_2 = H
6b (7*R*, 8*S*, 7'*R*, 8'*S*), R_1 = H, R_2 = H
8a (7*S*, 8*R*, 7'*S*, 8'*R*), R_1 = *β*-D-glu, R_2 = H
8b (7*R*, 8*S*, 7'*R*, 8'*S*), R_1 = *β*-D-glu, R_2 = H
10a (7*S*, 8*R*, 7'*S*, 8'*R*), R_1 = *β*-D-glu, R_2 = *β*-D-glu
10b (7*R*, 8*S*, 7'*R*, 8'*S*), R_1 = *β*-D-glu, R_2 = *β*-D-glu

Fig. 1 Structural sketches of all compounds mentioned.

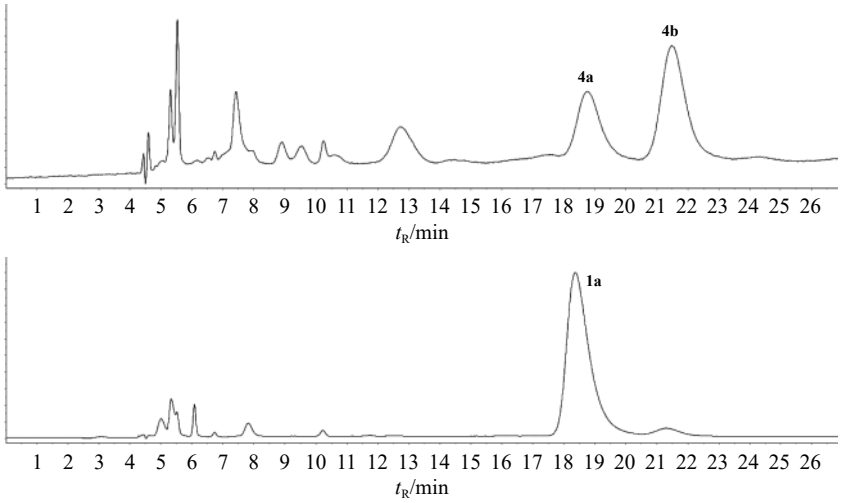

Fig. 2 Comparison of retention times of hydrolyzed aglycone fragments of 1a with 4a under the same HPLC condition.

ingaresinol-*O*-*β*-D-glucoside (7*S*,8*R*,7'*S*,8'*R*) (**7b**) [25]; (+)-eucommin A (7*S*,8*R*,7'*S*,8'*R*) (**8a**), (−)-eucommin A (7*R*,8*S*, 7'*R*,8'*S*) (**8b**) [26]; (+)-syringaresinol di-*O*-*β*-D-glucoside (7*S*, 8*R*,7'*S*,8'*R*) (**9a**), (−)-syringaresinol di-*O*-*β*-D-glucoside (7*R*, 8*S*,7'*R*,8'*S*) (**9b**) [27]; (+)-medioresinol di-*O*-*β*-D-glucopyranoside (7*S*,8*R*,7'*S*,8'*R*) (**10a**), and (−)-medioresinol di-*O*-*β*-D-glucopyranoside (7*R*,8*S*,7'*R*,8'*S*) (**10b**) [28]. These identifications were made by comparing the MS and 1D/2D NMR data with literature values and referencing the absolute configurations of the aglycone parts using ECD calculations, optical rotation values, and GC-MS analyses after hydrolysis derivatization.

In the present study, we observed that most carbon signals in the ^{13}C NMR spectra of the furofuran lignans and their derivatives exhibited twin peaks, even after high-temperature NMR experiments (60 °C), suggesting the presence of isomer pairs. Given that lignans typically exhibit enantiomeric properties [17], chiral resolution was subsequently performed. Thereafter, the ^{13}C NMR spectrum no longer displayed the twin peaks, and we isolated three types of compounds from the stems of *Dendrobium* 'Sonia', including furofuran lignan aglycones (**4**−**6**), monoglycosides (**1**−**3**, **7**−**8**), and diglycosides (**9**−**10**). Compounds **1**−**8** were directly obtained using a reverse chiral column, whereas compounds **9**−**10** were not

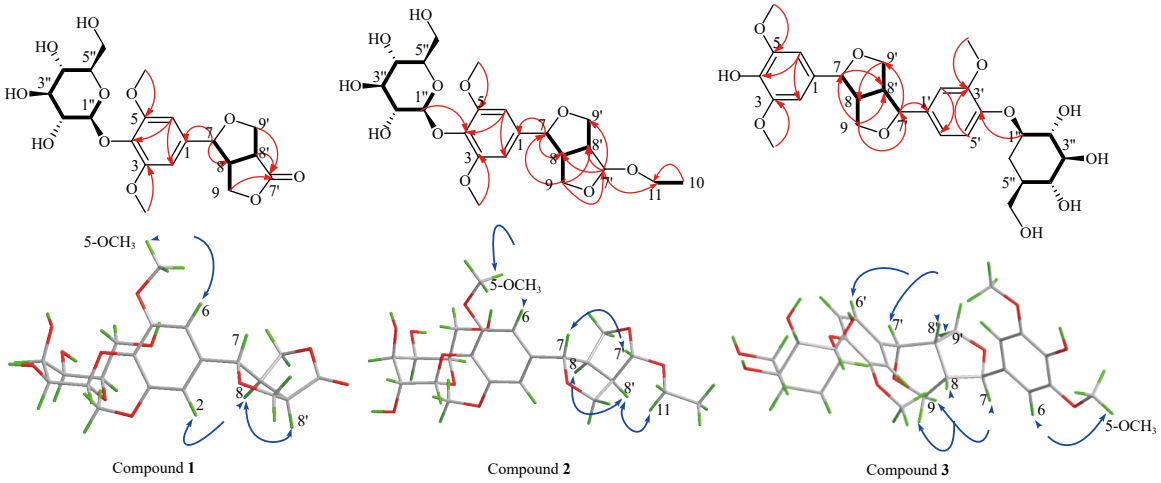

Fig. 3 Key HMBC (H⁀C), ^{1}H-^{1}H COSY (H—H), and NOESY (H⋯H) correlations of compounds 1–3.

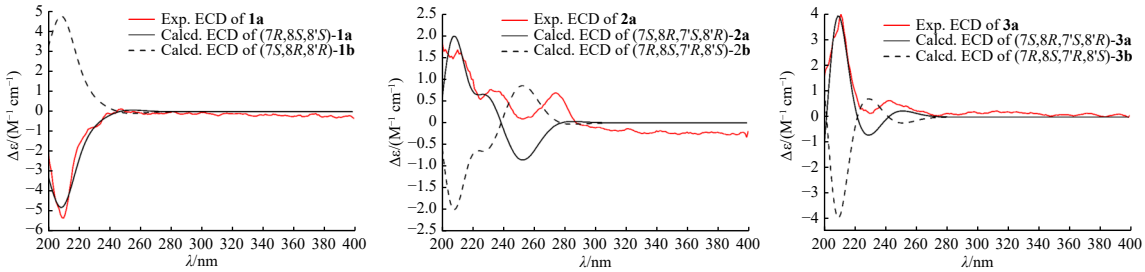

Fig. 4 Experimental and calculated ECD data for 1–3.

retained by the chiral column, and their final configurations were determined from the aglycone parts obtained after mild acid hydrolysis.

During the process of structure identification, we found an interesting pattern: CD curves showed negative peaks in the range of 200−250 nm and negative optical rotation values when the absolute configurations of the aglycone fragments were 7*R*, 8*S*, 8'*S*. Conversely, CD curves displayed positive peaks in the same range and positive optical rotation values when the absolute configurations were 7*S*, 8*R*, 8'*R* (Table 2). This finding could facilitate the stereochemical analysis of furofuran lignans and their derivatives in other plants.

Bioactivity evaluation

Compounds **1**−**9** were evaluated *in vitro* for their inhibitory activity against NO production in RAW264.7 cells. Aminoguanidine hydrochloride was used as a positive control. The results (Table 3) showed that syringaresinol (**5**) exhibited prominent anti-inflammatory activity with IC_{50} 27.7 ± 3.2 μmol·L^{-1}, closely matching previously reported values [12], suggests that syringaresinol may be the main anti-inflammatory component of *Dendrobium* 'Sonia'. There were slight differences in the activities of leveisomer **5a** (IC_{50} 26.9 ± 3.5 μmol·L^{-1}), dextroisomer **5b** (IC_{50} 35.5 ± 1.1 μmol·L^{-1}), and racemic **5** (IC_{50} 28.4 ± 3.0 μmol·L^{-1}). The other two groups of enantiomeric enantiomers **4a**, **4b** (IC_{50} > 100 μmol·L^{-1}) and **6a**, **6b** (IC_{50} > 50 μmol·L^{-1}) displayed slight anti-inflammatory activities. Overall, the results indicated that all the aglycones exhibited activity, whereas the glycosides did not. This lack of activity in the glycosides is likely attributable to their large molecular weight and strong hydrophilicity, resulting in poor drug-like properties.

Experimental

General experimental procedures

Optical rotations were measured on a Rudolph Research Analytical Autopol IV automatic polarimeter (Rudolph, New Jersey, USA). NMR spectra were recorded on a Bruker AV III spectrometer operating at 400 or 600 MHz (Bruker Corporation, Karlsruhe, Germany), with tetramethylsilane as an internal standard. HR-ESI-MS data were acquired on an Agilent 6546 series Q-TOF mass spectrometer (Agilent Technologies, Waldbronn, Germany). GC experiments were conducted using an Agilent 7890B instrument (Agilent Technologies, Waldbronn, Germany). CC was performed using D101 Macroporous resin (Tianjin SunLight Technology Co., Ltd., Tianjin, China), silica gel (200−300 mesh, Qingdao Marine Chemical Co., Ltd., Qingdao, China), and reversed-phase medium-pressure liquid chromatography (Buchi Labortechnik AG, Flawil, Switzerland) with a YMC-AQ gel ODS column (50 μm; YMC Co., Ltd., Kyoto, Japan). Additionally, Sephadex LH-20 (GE Healthcare Bio-Sciences AB, Uppsala, Sweden) was used for further separation. Thin-layer chromatography (TLC) was performed on glass plates precoated with silica gel (GF_{254}). Preparative HPLC was conducted using an LC3000 instrument (Beijing Chuangxintongheng Science and Technology Co., Ltd., Beijing, China) with a CAPCELL

Table 2 The absolute configuration, CD curve, and spin value of the aglycone parts of 1−7

No.	Absolute configuration	CD curve	Spin value
1a*	(7*R*, 8*S*, 8'*S*)	−	−59
2b*	(7*R*, 8*S*, 7'*R*, 8'*S*)	−	−52
3b*	(7*R*, 8*S*, 7'*R*, 8'*S*)	−	−101
4a	(7*R*, 8*S*, 8'*S*)	−	−39
5b	(7*R*, 8*S*, 7'*R*, 8'*S*)	−	−46
6b	(7*R*, 8*S*, 7'*R*, 8'*S*)	−	−19
7a	(7*R*, 8*S*, 7'*R*, 8'*S*)	−	−52
1b*	(7*S*, 8*R*, 8'*R*)	+	+50
2a*	(7*S*, 8*R*, 7'*S*, 8'*R*)	+	+67
3a	(7*S*, 8*R*, 7'*S*, 8'*R*)	+	0
4b	(7*S*, 8*R*, 8'*R*)	+	+40
5a	(7*S*, 8*R*, 7'*S*, 8'*R*)	+	+46
6a	(7*S*, 8*R*, 7'*S*, 8'*R*)	+	+13
7b	(7*S*, 8*R*, 7'*S*, 8'*R*)	+	+9

Notes: 1) A negative peak in the range of 200−250 nm of the CD curve was recorded as "−"; the opposite was recorded as "+"; 2) The structure numbering was unified as shown below.

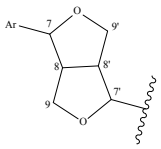

PAK C_{18}-AQ column (20mm × 250mm, 5 μm; SHISEIDO, Kyoto, Japan), a Cellu-JR chiral analytical column (4.6mm × 250mm, 5μm; Welch, Jinhua, China), a Cellu-JR chiral semi-preparative column (10 mm × 250 mm, 5 μm; Welch, Jinhua, China), a Chiral CD-Ph analytical column (4.6 mm × 250 mm, 5 μm; SHISEIDO, Kyoto, Japan) and a Chiral CD-Ph semi-preparative column (10 mm × 250mm, 5 μm; SHISEIDO, Kyoto, Japan). The CD curves were detected by a Chirascan circular dichroism instrument (Applied Photophysics Ltd., UK). The crystallographic data were collected on a Bruker d8 Venture system (Bruker, Germany).

Plant material

The dried stems of *Dendrobium* 'Sonia' were collected in January 2018 in Pu'er City, Yunnan Province. The plant material was identified as *Dendrobium* 'Sonia' of the Orchidaceae family by Prof. LI Yang (one of the authors). A voucher specimen (No. SNY20180107) was deposited at the Institute of Chinese Materia Medica, University of Traditional Chinese Medicine, Shanghai, China.

Extraction, isolation, and characterization

The air-dried stems of *Dendrobium* 'Sonia' (20 kg) were finely chopped and successively extracted with 95% EtOH (100 L) under reflux (2 × 2 h). The extract was then filtered, concentrated, and partitioned between H_2O and EtOAc, resulting in two distinct phases. The H_2O phase was subjected to

Table 3 Inhibitory effects of isolated compounds against NO production in RAW 264.7 cells (mean ± SD, *n* = 3)

Compound	IC_{50} (μmol·L^{-1})
4a	> 100
4b	> 100
5a	26.9 ± 3.5
5b	35.5 ± 1.1
5	28.4 ± 3.0
6a	> 50
6b	> 50
AG	27.3 ± 1.3

Note: 1) The samples showed cytotoxic effects to cells at > 100 μmol·L^{-1} (less than 75% cell survival). Other compounds tested did not demonstrate inhibitory effects; 2) AG = aminoguanidine hydrochloride.

CC using D101 macroporous resin as the stationary phase, with sequential elution using H_2O and 30%, 70%, and 95% EtOH (15 L each). The 30% ethanol eluate was fractionated by silica gel CC eluted with a gradient system of CH_2Cl_2−MeOH−H_2O (20 ∶ 1 ∶ 0 to 2 ∶ 1 ∶ 0.3), yielding nine factions (Frs. A−I) based on TLC analyses. Similarly, the 70% ethanol eluate was fractionated using a gradient system of CH_2Cl_2−MeOH−H_2O (10 ∶ 1 ∶ 0 to 2 ∶ 1 ∶ 0.3), resulting in three factions (Frs. J−L). The EtOAc phase was subjected to normal phase silica column chromatography, initially eluted with a gradient of PE−EtOAc (1 ∶ 0, 50 ∶ 1, 10 ∶ 1, 5 ∶ 1, 2 ∶ 1, 1 ∶ 1) and then with CH_2Cl_2−MeOH (100 ∶ 0, 90 ∶ 1, 70 ∶ 1, 50 ∶ 1, 20 ∶ 1, 10 ∶ 1, 5 ∶ 1, 3 ∶ 1, 2 ∶ 1, 1 ∶ 1, 1 ∶ 3, 0 ∶ 100). Each fraction was collected in 1 L volumes and concentrated under reduced temperature and pressure. Fractions with similar TLC profiles were combined to produce eight fractions (Frs. M−T).

Fr. B (6.1 g) was separated by preparative reverse-phase medium-pressure liquid chromatography (PR-MPLC) (MeOH−H_2O, 30 ∶ 70 to 100 ∶ 0), yielding thirteen fractions (Frs. B_{1-13}). Fr. B_2 was further purified by Sephadex LH-20 CC with MeOH−H_2O (4 ∶ 6) and subsequently by TLC and preparative HPLC using MeCN−H_2O as the mobile phase, yielding **2** (18 mg).

Fr. D (6.5g) (MeOH−H_2O, 20 ∶ 80 to 100 ∶ 0), Fr. F (5.5 g), and Fr. G (5.7 g) (MeOH−H_2O, 10 ∶ 90 to 100 ∶ 0) were subjected to PR-MPLC, resulting in Frs. D_{1-5}, Frs. F_{1-5}, and Frs. G_{1-4}. Fr. D_2 and Fr. G_1 were further purified by Sephadex LH-20 CC with MeOH−H_2O (3 ∶ 7) and subsequently by TLC and preparative HPLC using MeCN−H_2O as the mobile phase, yielding **1** (52 mg), **3** (8 mg), and **8** (5 mg). Fr. F_3 was enriched by Sephadex LH-20 CC and purified by preparative HPLC, yielding **7** (82 mg).

During the column chromatography of Fr. H, a large white precipitate formed. The solvent was removed by filtration, and the precipitate was washed to yield **9** (4 g).

Fr. I (7.0 g) was subjected to PR-MPLC (MeOH−H_2O,

0 ∶ 100 to 100 ∶ 0), yielding Fr. I_{1-2}. Fr. I_2 was purified by Sephadex LH-20 CC with MeOH−H_2O (3 ∶ 7) and subsequently by preparative HPLC, yielding **10** (20 mg).

Fr. R (48 g) was first eluted using MCI (MeOH−H_2O, 2 ∶ 8 to 1 ∶ 0) gradient, yielding eight fractions (Frs. R_{1-8}). Fr. R_7 was purified by Sephadex LH-20 (CH_2Cl_2−MeOH, 1 ∶ 1), followed by Sephadex LH-20 (MeOH) and subsequently by preparative HPLC, yielding **4** (10 mg).

Fr. T (90 g) was separated by MCI CC (MeOH−H_2O, 2 ∶ 8 to 1 ∶ 0) and TLC detection, yielding three fractions (Frs. T_{1-3}). Fr. T_2 was separated by MPLC (MeOH−H_2O, 5 ∶ 5 to 1 ∶ 0), yielding five subfractions Frs. T_{2a-2e}. Fr. T_{2d} was first separated by Sephadex LH-20 (MeOH), followed by preparative HPLC, yielding **5** (11 mg) and **6** (15 mg).

The chromatographic conditions were first mapped out on a conventional HPLC using a commercial chiral analytical column and then transferred to the preoperative HPLC instrument using the corresponding chiral semi-preparative column for preparation. Typically, the first eluted peak was designated as **a**, and the second as **b**. The column types and mobile phase rations used for the chiral resolution of each compound were as follows: **1** (CD-Ph, MeCN−H_2O, 10 ∶ 90), **2** (Cellu-JR, MeCN−MeOH−H_2O, 8 ∶ 2 ∶ 90), **3** (CD-Ph, MeCN−H_2O, 20 ∶ 80), **4** (Cellu-JR, MeOH−H_2O, 67 ∶ 33), **5** (Cellu-JR, MeCN−H_2O, 33 ∶ 67), **6** (Cellu-JR, MeCN−H_2O, 32 ∶ 68), **7** (CD-Ph, MeCN−H_2O, 24 ∶ 76), **8** (CD-Ph, MeCN−H_2O, 20 ∶ 80). However, **9** and **10** were not retained within the chiral columns due to their high polarity, which hindered effective chiral separation. Consequently, chiral preparation for these compounds was not achieved.

Compound 1a, White solid; $[\alpha]_D^{20}$ −59.2 (*c* 0.1, MeOH); UV (MeOH) λ_{max} (nm): 206, 238; IR ν_{max}: 3352, 2916, 1763, 1593, 1122, 1014, 952.4, 832 cm^{-1}; ^1H NMR and ^{13}C NMR spectroscopic data (Table 1); HR-ESI-MS *m/z* 441.1401 $[M - H]^-$ (Calcd. for $C_{20}H_{26}O_{11}$, 441.1402).

Compound 1b, White solid; $[\alpha]_D^{20}$ + 49.5 (*c* 0.1, MeOH); UV (MeOH) λ_{max} (nm): 206, 238; IR ν_{max}: 3352, 2916, 1763, 1593, 1122, 1014, 952.4, 832 cm^{-1}; ^1H NMR and ^{13}C NMR spectroscopic data (Table 1); HR-ESI-MS *m/z* 441.1401 $[M - H]^-$ (Calcd. for $C_{20}H_{26}O_{11}$, 441.1402).

Compound 2a, White solid; $[\alpha]_D^{20}$ + 67.3 (*c* 0.1, MeOH); UV (MeOH) λ_{max} (nm): 206, 231; IR ν_{max}: 3330, 1595, 1482, 1040 cm^{-1}; ^1H NMR and ^{13}C NMR spectroscopic data (Table 1); HR-ESI-MS *m/z* 471.1876 $[M - H]^-$ (Calcd. for $C_{22}H_{31}O_{11}$, 471.1871).

Compound 2b, White solid; $[\alpha]_D^{20}$ −51.6 (*c* 0.1, MeOH); UV (MeOH) λ_{max} (nm): 206, 231; IR ν_{max}: 3330, 1595, 1482, 1040 cm^{-1}; ^1H NMR and ^{13}C NMR spectroscopic data (Table 1); HR-ESI-MS *m/z* 471.1876 $[M - H]^-$ (Calcd. for $C_{22}H_{31}O_{11}$, 471.1871).

Compound 3b, White solid; $[\alpha]_D^{20}$ −100.6 (*c* 0.1, MeOH); UV (MeOH) λ_{max} (nm): 209, 230; IR ν_{max}: 3355, 2937, 1610, 1514, 1219, 1054, 1033, 824 cm^{-1}; ^1H NMR and ^{13}C NMR spectroscopic data (Table 1); HR-ESI-MS *m/z* 549.1980 $[M - H]^-$ (Calcd. for $C_{27}H_{34}O_{12}$, 549.1977).

The crystallographic data of two known compounds have been deposited at the Cambridge Crystallographic Data Center (CCDC 2277660 for **5a**, 2277661 for **6b**). Detailed data can be accessed for free at http://www.ccdc.cam.ac.uk.

Acid hydrolysis derivatization reaction

The derivatization conditions were optimized based on established literature protocols [29]. Each glycoside compound (1 mg) was hydrolyzed with 2 $mol \cdot L^{-1}$ trifluoroacetic acid (1 mL) at 120 °C for 2 h and then evaporated under vacuum. The resulting hydrolysates were treated accordingly and analyzed by GC-MS. These optimized conditions enabled baseline separation of D/L-glucose derivatization products. The residue peak for D-glucose was detected at 43.05 min, as confirmed by comparison with an authentic sample.

Cell viability test

RAW 264.7 cells were cultured in a DMEM medium supplemented with 10% fetal bovine serum, 100 $U \cdot mL^{-1}$ penicillin, and 100 $\mu g \cdot mL^{-1}$ streptomycin. The cells were incubated at 37 °C in a humidified atmosphere with 5% CO_2. After reaching the desired confluence, the cells were treated with the DMEM solution containing various concentrations of each test compound or an equivalent concentration of DMSO, followed by incubation under the same conditions for over 22 h. The cell viability was assessed using the Cell Counting Kit-8 kit according to the manufacturer's instructions. The OD value was measured at 450 nm with a microplate reader, and the cytotoxicity was evaluated according to the formula.

NO inhibitory assay

The adherent Raw 264.7 cells were incubated for 24 h with different concentrations of each test compound, dissolved in DMSO in the presence of LPS. Nitrite, an indicator of NO production, was measured using the Griess reaction [30], and the absorbance was measured at 540 nm using a microplate reader. Each dosing group was 3 in parallel and all experiments were conducted in triplicate.

ECD calculation details

Conformational analyses were conducted *via* random searching in the Sybyl-X 2.0 using the MMFF94S force field with an energy cutoff of 5 $kcal \cdot mol^{-1}$. This process identified the five lowest energy conformers. Subsequent geometry optimizations and frequency analyses were performed at the B3LYP-D3(BJ)/6-31G* level in CPCM methanol using ORCA5.0.1. All conformers used for property calculations were confirmed to be stable points on the potential energy surface (PES) with no imaginary frequencies. The excitation energies, oscillator strengths, and rotational strengths (velocity) of the first 60 excited states were calculated using the time-dependent density functional theory (TD-DFT) methodology at the PBE0/def2-TZVP level in CPCM methanol using ORCA5.0.1. The ECD spectra were simulated by the overlapping Gaussian function (half the bandwidth at 1/e peak height, sigma = 0.30 for all) [31]. Gibbs free energies for the conformers were calculated using thermal corrections at the B3LYP-D3(BJ)/6-31G* level, and electronic energies

were evaluated at the wB97M-V/def2-TZVP level in CPCM methanol using ORCA5.0.1. The final spectra were obtained by averaging the simulated spectra of the conformers according to Boltzmann distribution theory based on their relative Gibbs free energy (ΔG). By comparing the experiment spectra with the calculated spectra of model molecules, the absolute configuration of the only chiral center was determined.

Supplementary Information

NMR, MS, IR, GC-MS analysis, X-ray single, CD curves and experimental chiral resolution data are available as Supporting Information, and can be requested by sending E-mails to the corresponding author.

References

[1] Ren G, Deng WZ, Xie YF, *et al*. Bibenzyl derivatives from leaves of *Dendrobium officinale* [J]. *Nat Prod Commun*, 2020, **15**(2):1-5.

[2] Shang ZM, Li XF, Xiao SJ. Two new bibenzyl compounds from *Dendrobium lindleyi* [J]. *Rec Nat Prod*, 2020, **14**(6): 416-420.

[3] Wu LL, Lu Y, Ding YL, *et al*. Four new compounds from *Dendrobium devonianum* [J]. *Nat Prod Res*, 2019, **33**(15): 2160-2168.

[4] Chen YG, Yu H, Lian X. Isolation of stilbenoids and lignans from *Dendrobium hongdie* [J]. *Trop J Pharm Res*, 2015, **14**(11): 2055-2059.

[5] Ye QH, Zhao WM, Qin GW. Lignans from *Dendrobium chrysanthum* [J]. *J Asian Nat Prod Res*, 2004, **6**(1): 39-43.

[6] Wang P, Chen X, Wang H, *et al*. Four new picrotoxane-type sesquiterpenes from *Dendrobium nobile* Lindl [J]. *Front Chem*, 2019, **7**: 812.

[7] Yang L, Zhang CF, Yang H, *et al*. Two new alkaloids from *Dendrobium chrysanthum* [J]. *Heterocycles*, 2005, **65**(3): 633-636.

[8] Yu W, Ren Z, Zhang X, *et al*. Structural characterization of polysaccharides from *Dendrobium officinale* and their effects on apoptosis of HeLa cell line [J]. *Molecules*, 2018, **23**(10): 2484.

[9] Chang CC, Ku AF, Tseng YY, *et al*. 6, 8-Di-*C*-glycosyl flavonoids from *Dendrobium huoshanense* [J]. *J Nat Prod*, 2010, **73**(2): 229-232.

[10] Liang ZY, Zhang JY, Huang YC, *et al*. Identification of flavonoids in *Dendrobium huoshanense* and comparison with those in allied species of *Dendrobium* by TLC, HPLC and HPLC coupled with electrospray ionization multi-stage tandem MS analyses [J]. *J Sep Sci*, 2019, **42**(5): 1088-1104.

[11] Poobathy R, Sinniah UR, Xavier R, *et al*. Catalase and superoxide dismutase activities and the total protein content of protocorm-like bodies of *Dendrobium* Sonia-28 subjected to vitrification [J]. *Appl Biochem Biotechnol*, 2013, **170**(5): 1066-1079.

[12] Cai BX, Song LX, Hu HJ, *et al*. Structures and biological evaluation of phenylpropanoid derivatives from *Dendrobium* Sonia [J]. *Nat Prod Res*, 2021, **35**(23): 5120-5124.

[13] Qiu H, Song LX, Yang YB, *et al*. Two new stilbenoid diglycosides from the stems of *Dendrobium* 'Sonia' [J]. *J Asian Nat Prod Res*, 2023, **25**(3): 245-251.

[14] Polat Kose L, Gulcin İ. Evaluation of the antioxidant and anti-radical properties of some phyto and mammalian lignans [J]. *Molecules*, 2021, **26**(23): 7099.

[15] Zou YY, Wang DW, Yan YM, *et al*. Lignans from *Lepidium meyenii* and their anti-inflammatory activities [J]. *Chem Biodivers*, 2021, **18**(8): e2100231.

[16] Favela-Hernández JMJ, García A, Garza-González E, *et al*. Antibacterial and antimycobacterial lignans and flavonoids from *Larrea tridentata* [J]. *Phytother Res*, 2012, **26**(12): 1957-1960.

[17] Smeds AI, Eklund PC, Willför SM. Content, composition, and stereochemical characterisation of lignans in berries and seeds [J]. *Food Chem*, 2012, **134**(4): 1991-1998.

[18] Katayama Y, Fukuzumi T. Formation of new acetal linkages in the metabolism of syringaresinol structure of lignin by *Coriolus versicolor* [J]. *FEMS Microbiol Lett*, 1989, **58**(2): 247-253.

[19] Sugiyama MKM. Studies on the constituents of *Osmanthus* species. VII. structures of lignan glycosides from the leaves of *Osmanthus asiaticus* Nakai [J]. *Chem Pharm Bull*, 1991, **39**(2): 483-485.

[20] Saladino R, Fiani C, Crestini C, *et al*. An efficient and stereoselective dearylation of asarinin and sesamin tetrahydrofurofuran lignans to acuminatolide by methyltrioxorhenium/H_2O_2 and UHP systems [J]. *J Nat Prod*, 2007, **70**(1): 39-42.

[21] Zhou XM, Zheng CJ, Wu JT, *et al*. Five new lactone derivatives from the stems of *Dendrobium nobile* [J]. *Fitoterapia*, 2016, **115**: 96-100.

[22] Ma CM, Nakamura N, Min BS, *et al*. Triterpenes and lignans from *Artemisia caruifolia* and their cytotoxic effects on meth-A and LLC tumor cell lines [J]. *Chem Pharm Bull*, 2001, **49**(2): 183-187.

[23] Chiba K, Yamazaki M, Umegaki E, *et al*. Neuritogenesis of herbal (+)- and (−)-syringaresinols separated by chiral HPLC in PC12h and Neuro2a cells [J]. *Biol Pharm Bull*, 2002, **25**(6): 791-793.

[24] Li P, Zuo TT, Wang XQ, *et al*. Chemical constituents of *Scutellaria barbata* D. Don (II) [J]. *Chin J Med Chem*, 2008, **18**(5): 374-376.

[25] Wang CZ, Jia ZJ. Lignan, phenylpropanoid and iridoid glycosides from *Pedicularis torta* [J]. *Phytochemistry*, 1997, **45**(1): 159-166.

[26] Tolstikhina VV, Semenov AA, Ushakov IA. Minor furofuranoid lignans from cultivated cells of *Scorzonera hispanica* L. [J]. *Rastit Resur*, 1999, **35**(1): 87-90.

[27] Yamaguchi H, Nakatsubo F, Katsura Y, *et al*. Characterization of (+) and (−)-syringaresinol di-*β*-D-glucosides [J]. *Holzforschung*, 1990, **44**(5): 381-385.

[28] Deyama, Takeshi. The constituents of *Eucommia ulmoides* Oliv. I. Isolation of (+)-medioresinol di-*O*-*β*-D-glucopyranoside [J]. *Chem Pharm Bull*, 1983, **31**(9): 2993-2997.

[29] Navarro DA, Stortz CA. Determination of the configuration of 3,6-anhydrogalactose and cyclizable *α*-galactose 6-sulfate units in red seaweed galactans [J]. *Carbohydr Res*, 2003, **338**(20): 2111-2118.

[30] Schmölz L, Wallert M, Lorkowski S. Optimized incubation regime for nitric oxide measurements in murine macrophages using the Griess assay [J]. *J Immunol Methods*, 2017, **449**: 68-70.

[31] Stephens PJ, Harada N. ECD cotton effect approximated by the Gaussian curve and other methods [J]. *Chirality*, 2010, **22**(2): 229-233.

Cite this article as: QIU Kaimei, QIU Hao, XIE Yanqiao, *et al*. Chiral resolution of furofuran lignans and their derivatives from the stems of *Dendrobium* 'Sonia' [J]. *Chin J Nat Med*, 2024, **22**(10): 937-944.